JOURNAL OF MATERIALS SCIENCE 28 (1993) 735–741

Thermal shock resistance of SiC fibre-reinforced borosilicate glass and lithium aluminosilicate matrix composites

Y. KAGAWA
Institute of Industrial Science, The University of Tokyo, 7-22-1, Roppongi, Minato-ku, Tokyo 106, Japan

N. KUROSAWA*, T. KISHI
Research Centre for Advanced Science and Technology (RCAST), The University of Tokyo, 4-6-1, Komaba, Meguro-ku, Tokyo 153, Japan

Thermal shock resistance of an SiC fibre-(Nicalon®) reinforced borosilicate glass (Pyrex) and lithium aluminosilicate (LAS) matrix composite has been investigated experimentally in the temperature range 0–1000 K. Longitudinal Young's modulus and flexure strength of the composites after thermal shock were obtained as a function of thermal shock temperature. The results are discussed with the observed damage of the composite. The borosilicate glass matrix composite showed multiple cracking of the glass matrix perpendicular to the fibre axis when the thermal shock temperature was above 600 K. Decreases in Young's modulus and flexure strength were also recognized after multiple cracking of the matrix was initiated. On the other hand, the LAS matrix composite showed no damage at thermal shock temperatures below 800 K. However, at 800 K and above, microcracking of the matrix along the fibre axis was observed. After thermal shock, no decrease in the flexure strength was recognized, while the Young's modulus decreased due to microcracking of the matrix when the thermal shock temperatures were 800 K and above. It was found that the major advantage of the composite against thermal shock was to retain non-catastrophic failure properties even after the development of thermally induced damage in the composite.

1. Introduction

Recently, properties of fibre-reinforced ceramic matrix composites have been extensively studied [1–4]. The composites exhibit superior mechanical properties, such as strength, toughness, and/or work of fracture, up to elevated temperatures, and the materials are also expected to have application as high-temperature use structural materials. In such a case, the composite materials are often subjected to thermal shock conditions. Therefore, it is necessary to have a clear understanding of the degradation behaviour of composites due to thermal shock before application. However, little information is available about thermal shock behaviour of continuous fibre-reinforced ceramics. Mazdiyasni and Ruh [5] tested fracture experiments on thermal-shocked BN fibre-reinforced Si_3N_4 matrix composites and found a lower tendency for the catastrophic failure behaviour of the composite compared with monolithic ceramics. Yang *et al.* [6] carried out thermal shock experiment on three - dimensional braided SiC fibre-reinforced SiC after holding it for a long time at high temperature, and found superior thermal shock resistance of the composite. More recently, Long *et al.* [7] reported some experimental results on thermal shock resistance of SiC fibre-reinforced cordielite matrix composites and found high-temperature thermal shock resistance of the composite.

These papers show that thermal shock resistance of the composites is excellent compared with the unreinforced monolithic matrix materials. However, for a clear understanding of the thermal shock behaviour in fibre-reinforced ceramics, more detailed information is required. In this work, attention was focused on the thermal shock behaviour of SiC fibre-reinforced borosilicate glass and LAS matrix composite, because these composites have good mechanical properties and the composites are candidates for elevated temperature structural applications.

2. Experimental procedure

Unidirectionally reinforced continuous SiC fibre (Nicalon, Nippon Carbon Co. Ltd., Japan) -reinforced borosilicate glass (Corning Glass Works, Code 7740, Pyrex) and LAS (Li_2O_3–Al_2O_3–SiO_2 base glass

* *Present address*: Kawasaki Steel Corporation, Japan.

0022–2461

ceramics) matrix composites with fibre volume fractions of 0.5 and 0.4, respectively, were used. The chemical composition of LAS matrix was very similar in composition to Corning 9608 glass ceramics; however, ZrO_2 replaced the TiO_2 and approximately 5 wt % Nb_2O_5 was added in the LAS matrix. The composite material was fabricated by a conventional vacuum hot-pressing process and details of the processing variables have already been reported [8]. In the LAS matrix composite, as-hot-pressed composite was used without further ceraming.

The composite was machined to bar-type specimens using diamond-edge wheel blades. The dimensions of the bar type specimens were 2.0 mm × 2.0 mm × 40.0 mm. The surface of the specimen was finally polished with 0.2 μm diamond paste. Borosilicate glass bars, in which the dimensions were the same as those of the composite, were cut and polished from borosilicate glass plate (Corning Glass Works, Code 7740, Pyrex) for comparison of thermal shock resistance.

The apparatus used for the thermal shock experiment is illustrated in Fig. 1. The specimen was put on to a stainless steel holder and was located in a silica tube. The sample was located at the centre of an infrared furnace and the temperature of the sample was measured using a Pt–Rh type thermocouple in contact with a stainless steel sleeve covered the outside of the silica tube to avoid temperature distribution in the specimen. For the thermal shock test, the specimen was heated to a given temperature at a rate of 100 K min^{-1} and held for 10 min, and then rapidly quenched in cold water (290 K). In this experiment, the maximum holding temperature was 1290 K, which corresponded to the thermal shock temperature of 1000 K. The thermal shock experiments were carried out at holding temperatures from 0–1290 K which corresponded to thermal shock temperatures, ΔT, from 0–1000 K ($\Delta T = 0$ K is the non-thermal-shocked condition).

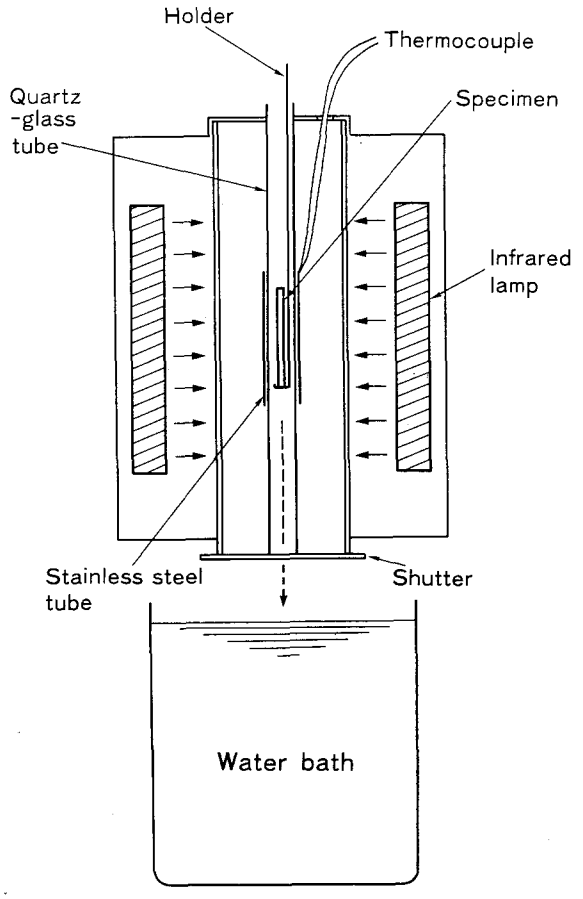

Figure 1 Schematic drawing of the experimental apparatus.

After the thermal shock test, the morphology of the thermally shocked specimen was observed by optical microscopy to examine damage characteristics. Reflective and Nomarski interference mode were used according to the condition of surface.

Three-point flexure tests of the both unshocked and thermally-shocked composite were carried out using an Instron testing machine with a span length of 30 mm. The tests were carried out in air at 297 K with a crosshead speed of 0.04 mm min^{-1}. The flexural strength was obtained from the maximum load of the load–displacement curve. Young's modulus of the composite was obtained from the load–displacement curve after calibration of the stiffness of the fixture and testing machine using a stiff SiC bar.

3. Results and discussion

3.1. SiC fibre-reinforced borosilicate glass matrix

Fig. 2 shows a typical surface of the non-thermally shocked (a), and thermally-shocked composite (b–d) specimens at different thermal shock temperatures. Multiple cracking was observed clearly in the glass matrix perpendicular to the fibre axis above thermal shock temperatures of 600 K. This multiple cracking behaviour is the same as that observed in the tensile test of fibre-reinforced brittle matrix composites [9]. Fig. 3 shows the distribution of spacing between cracks obtained from the specimens with $\Delta T = 700$ and 800 K. The spacing between the cracks of the matrix increased with increasing thermal shock temperature. As-thermally shocked and slightly polished surfaces of the thermally-shocked composite, with $\Delta T = 700$ and 800 K, respectively, are shown in Fig. 4 a–d. After slightly polishing the surface (30–40μm), the multiple cracking of the borosilicate glass matrix completely disappeared. This result suggests that the depths of the cracks were independent of the thermal shock temperature and were as long as two or three fibre diameters. When the thermal shock temperatures were below 600 K, no visible damage was recognized at the surface of the composite.

Fig. 5 shows typical three-point flexure load–displacement curves for as-hot-pressed and thermally-shocked composites with $\Delta T = 800$ K. In both specimens, the load increased linearly in the initial stage. After the linear region near the origin, the curve of the non-thermally-shocked composite exhibited a non-linear load–displacement relation which corresponded to cracking of matrix and fibre fracture at the tensile surface of the composite specimen. The load–displacement relation of the thermally-shocked composite specimen was completely different from

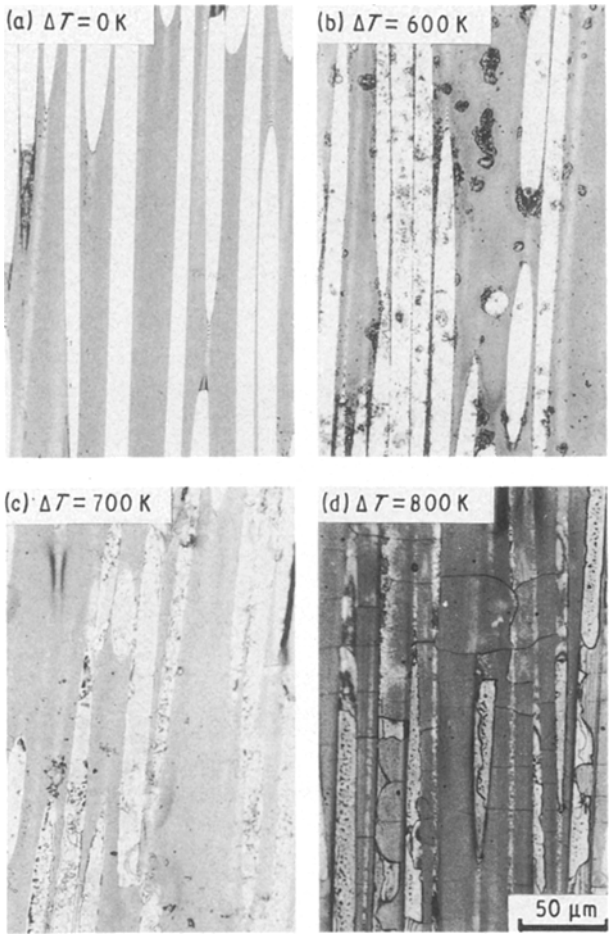

Figure 2 Typical optical micrographs of surface of the SiC fibre-reinforced borosilicate glass matrix composite (a) before and (b–d) after thermal shock at ΔT 600 K, (c) 700 K and (d) 800 K.

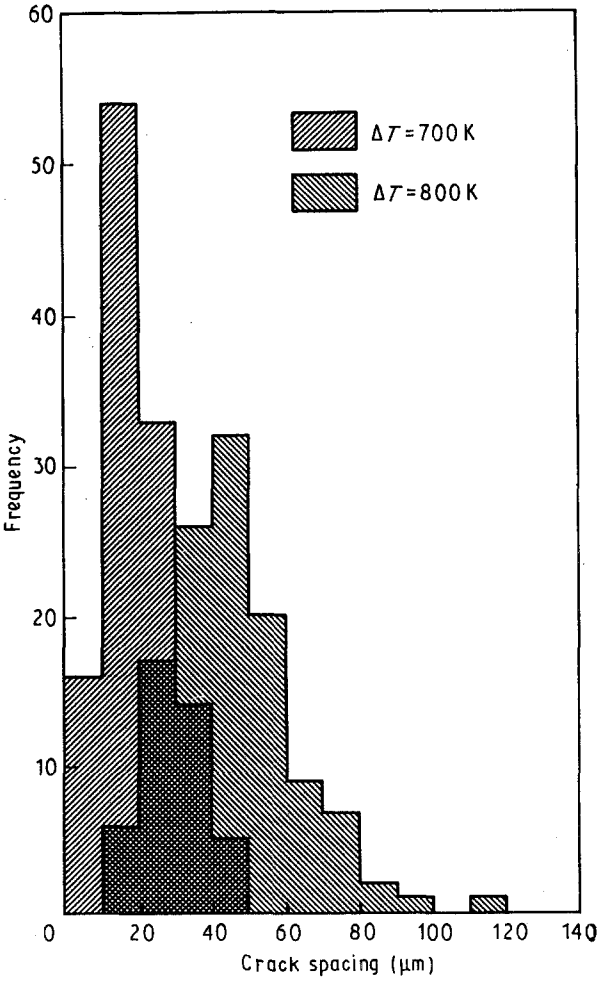

Figure 3 Distribution of crack-to-crack spacing for thermally shocked SiC fibre-reinforced borosilicate glass matrix composite with ΔT = 700 and 800 K.

that of the non-thermally-shocked composite specimen. In this case, after the linear part, a step-wise load drop was observed, the sudden load drop being due to interlaminar shear failure of the specimen near the neutral plane, as shown in Fig. 6. This type of load drop was repeated until a sudden drop of the load.

Fig. 7 shows plots of longitudinal elastic modulus versus the thermal shock temperature, ΔT. The longitudinal Young's modulus of the composite was obtained from the load–displacement relation. When the thermal shock temperature was lower than 600 K, the Young's modulus after a thermal shock had the same value of the original non-thermal shocked composite. However, when the thermal shock temperatures were above 600 K, the Young's modulus of the heat-shocked composite decreased with increasing thermal shock temperature. This seems to be attributable to the multiple cracking of the borosilicate glass matrix. Although multiple cracking of the matrix occurred, the composite required about a 100 K higher thermal shock temperature for damage initiation than the unreinforced borosilicate glass.

The change in the three-point flexure strength of the composite specimen with thermal shock temperature is shown in Fig. 8. The maximum three-point flexure strength was obtained from the maximum load of the load–displacement curve. At thermal shock temperatures of 500 K and below, the flexure strength of the thermally-shocked composite gradually increased with thermal shock temperature. The increase in the flexure strength may be related to the decrease in surface flow in the matrix by viscous flow of the borosilicate glass matrix during holding at high temperatures. When the thermal shock temperatures were above 600 K, the flexure strength of the thermally-shocked composite decreased with increasing thermal shock temperature. The decrease of the flexure strength was probably due to the change of failure modes which arose from change of interfacial shear strength. This strength versus thermal shock temperature relation is completely different from the unreinforced borosilicate glass. Because the thermally shocked composites tend to fracture by interlaminar shear failure, as shown in Fig. 6, and if interlaminar fracture is initiated, the flexure load cannot increase in the case of composites without interlaminar fracture.

3.2. SiC fibre-reinforced LAS matrix composite

Fig. 9 shows the typical surface appearance of the non-thermally shocked (a), and thermally-shocked (b–d) specimens with applied thermal shock temperature. The white parts in the figure indicate SiC fibre

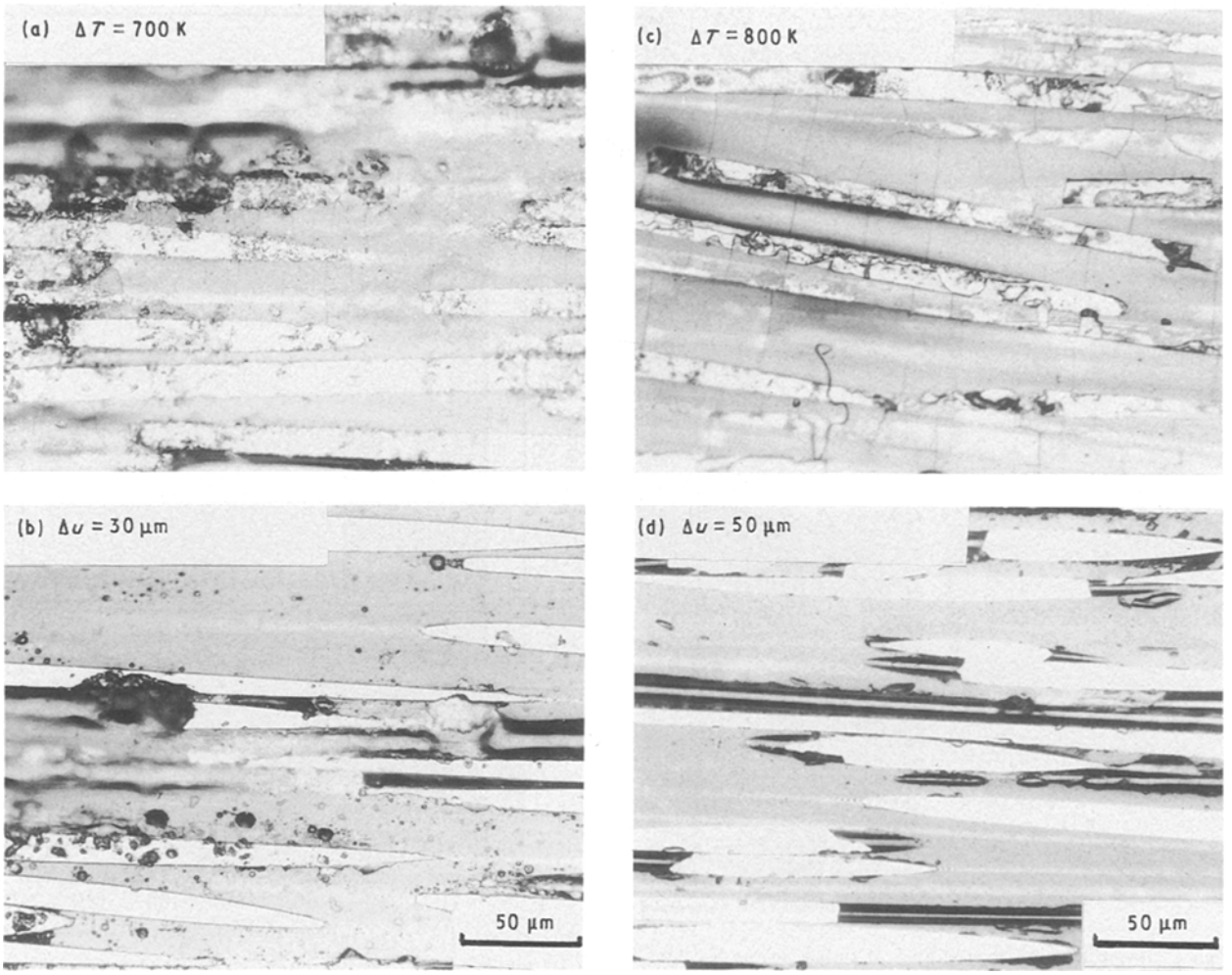

Figure 4 Typical optical micrographs of (a, b) as-thermally shocked and (c, d) polished surface of SiC fibre-reinforced borosilicate glass matrix composite. The thermal shock temperature, ΔT, and polished depth, Δu, are indicated.

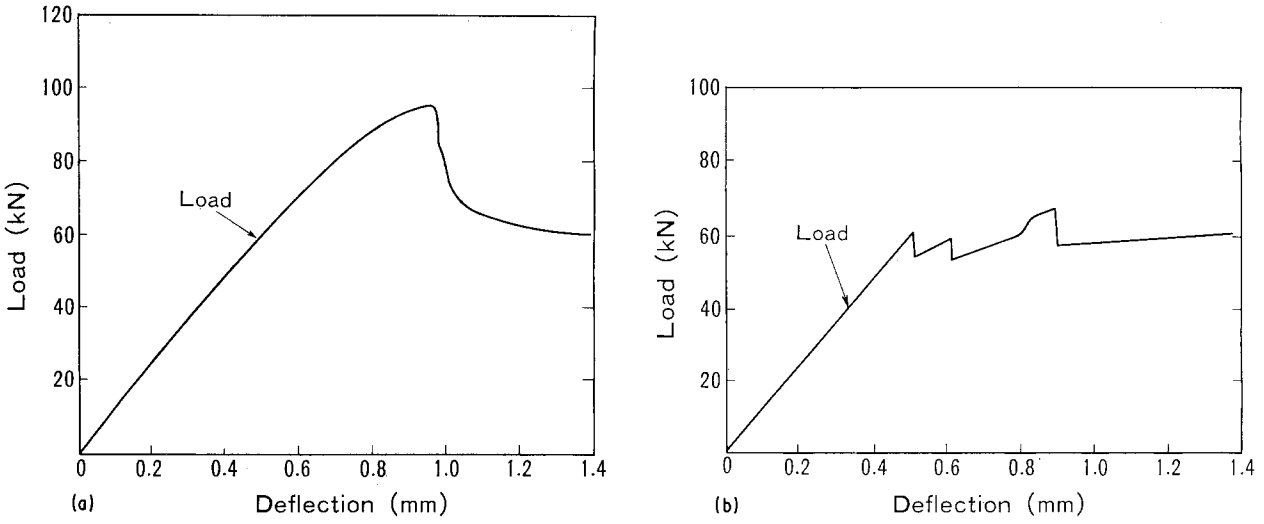

Figure 5 Typical three-point flexure load–displacement curves for (a) non-thermally shocked SiC fibre-reinforced borosilicate glass matrix composite and (b) thermally-shocked composite with $\Delta T = 800$ K.

and the grey area indicates LAS matrix. When the thermal shock temperature, ΔT, was 600 K and above, a needle-like crystalline structure, shown in Fig. 10, was observed in the LAS matrix. A typical X-ray diffraction result is shown in Fig. 10. X-ray diffraction results indicated the needle-like structure (Fig. 9b–d) was considered to be due to the formation of β-spodumen-silica solid solution ($(Li_2O, MgO) \cdot Al_2O_3 \cdot nSiO_2$ ($n > 3.5$)) by crystallization of the LAS matrix, while the specimen was held at a thermal shock temperature higher than 600 K. The remaining matrix probably consists of continuous glassy grain-boundary phase plus small crystals of mullite ($3Al_2O_3 \cdot 2SiO_2$) and zircon ($ZrSiO_4$) [10, 11].

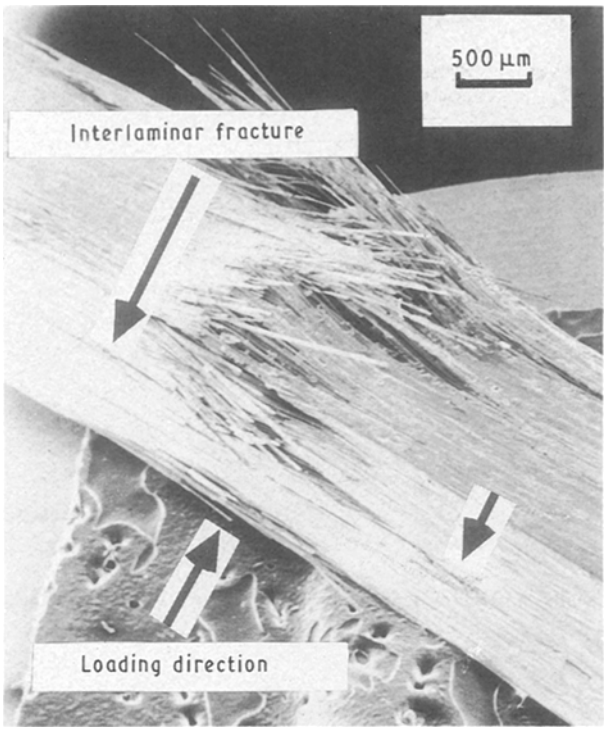

Figure 6 Scanning electron micrograph of typical three-point fracture appearance of the SiC fibre-reinforced borosilicate glass composite after thermal shock ($\Delta T = 800$ K).

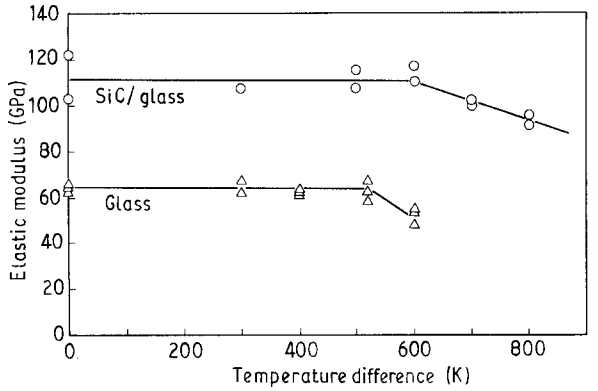

Figure 7 Plots of longitudinal Young's modulus versus thermal shock temperature for SiC fibre-reinforced borosilicate glass and unreinforced borosilicate glass.

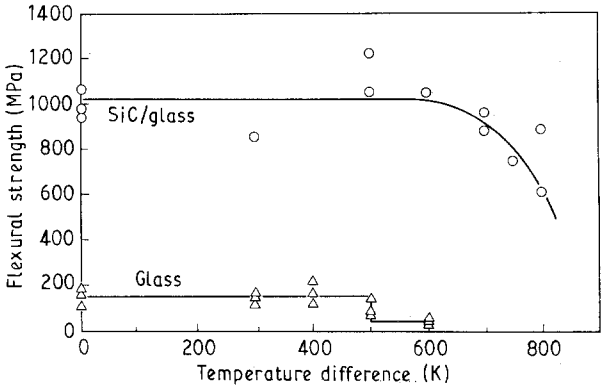

Figure 8 Plots of three-point flexure maximum stress-versus thermal shock temperature for SiC fibre-reinforced borosilicate glass and unreinforced borosilicate glass.

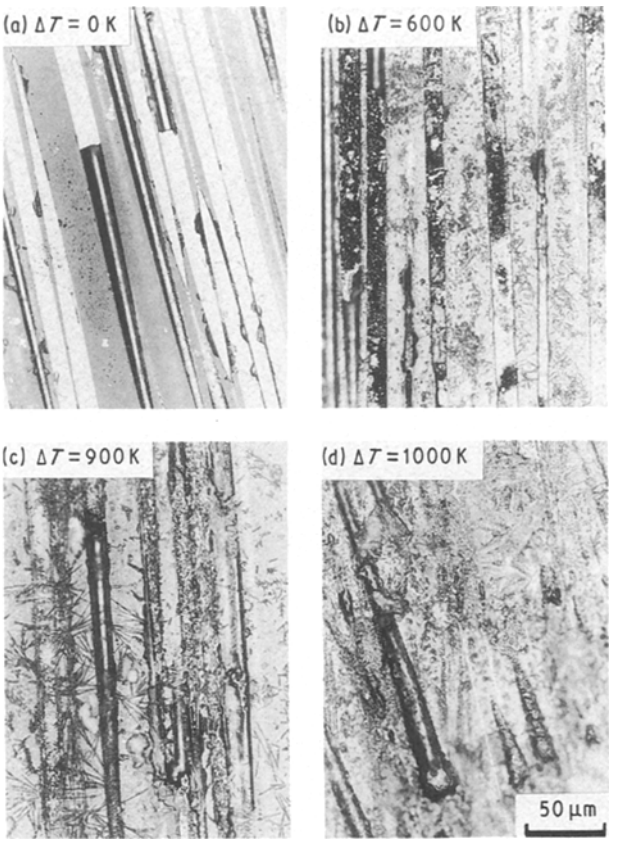

Figure 9 Typical optical micrographs of surface of the SiC fibre-reinforced LAS matrix composite (a) before and (b–d) after thermal shock.

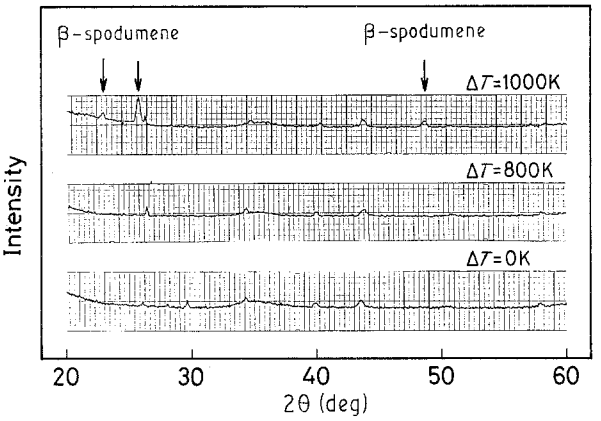

Figure 10 X-ray diffraction profiles for heat-exposed (10 min) SiC fibre-reinforced LAS matrix composites.

Fig. 11 shows detail of the microcracking in the matrix observed in the SiC fibre-reinforced LAS matrix composite with $\Delta T = 1000$ K. The same microcracking of the matrix was observed in all the specimens tested at $\Delta T = 800$ K and above. Most of the microcrackings, shown in Fig. 11, were located along the fibre axis direction. However, the microcracks formed were as long as two or three fibre diameters in the through-thickness direction, as in the case of borosilicate glass matrix. In the matrix rich region, especially, microcracks were seen around the formed β-spodumen and this behaviour is shown in Fig. 12. This evidence suggests that the anisotropic properties of β-spodumen can act as a source of microcracking

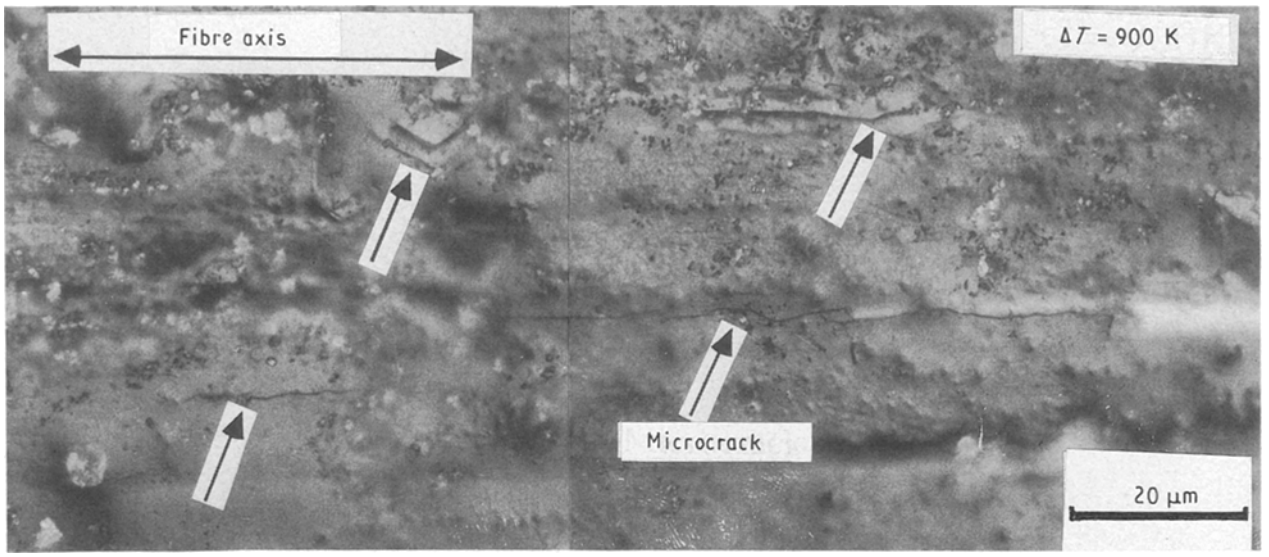

Figure 11 Appearance of microcracking observed in the surface of the thermally-shocked SiC fibre-reinforced LAS matrix composite with ΔT = 1000 K (Nomarski interference micrograph).

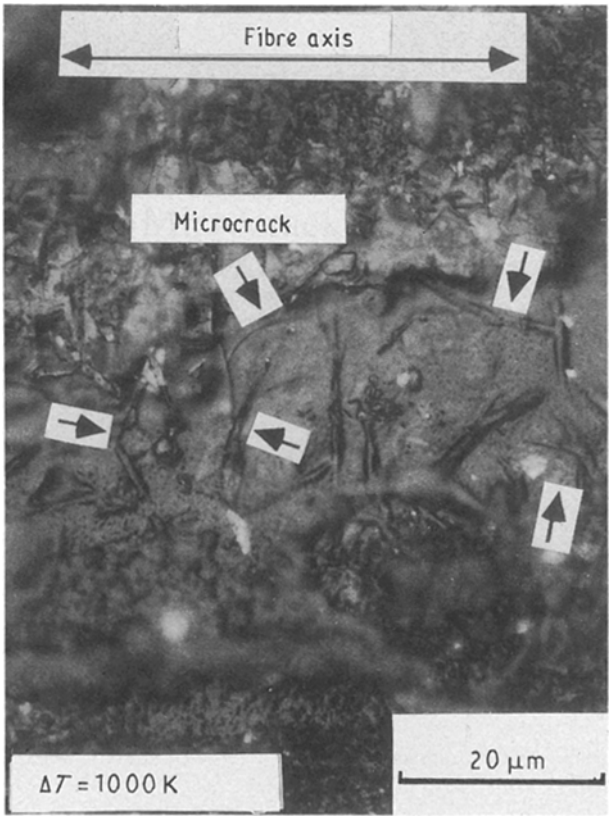

Figure 12 Appearance of microcracking observed in the surface of the heat-shocked SiC fibre-reinforced LAS matrix composite near the matrix-rich region with ΔT = 1000 K (Nomarski interference micrograph).

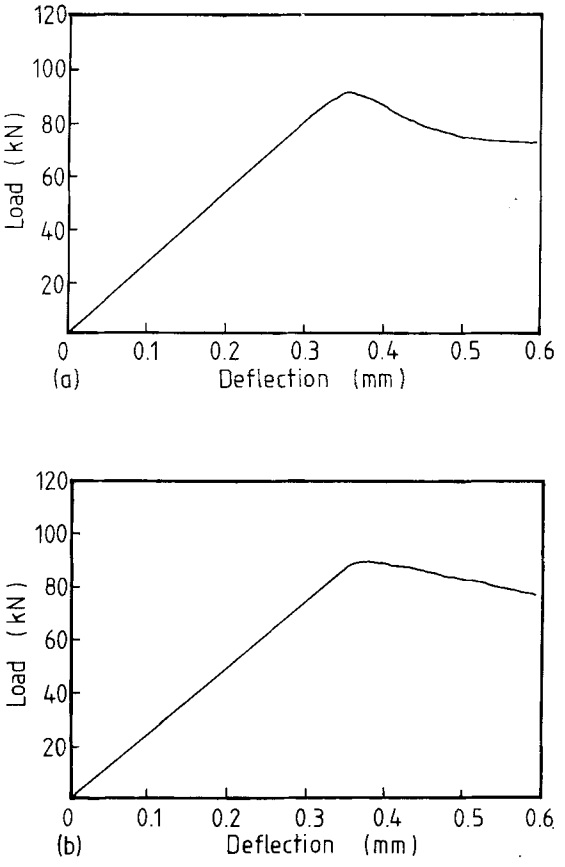

Figure 13 Typical three-point flexure load–displacement curves for (a) non-thermally shocked SiC fibre-reinforced LAS matrix composite and (b) the thermally-shocked composite with ΔT = 800 K.

because of thermal expansion anisotropy in the *a*- and *c*- directions. This spread of a damage zone only near the surface is similar to the case of SiC fibre-reinforced borosilicate glass. However, in the case of a borosilicate matrix composite, multiple cracking of the matrix perpendicular to the fibre axis was observed and the difference is probably due to thermal shock resistance of the LAS matrix.

Typical three-point flexure load–displacement curves for non-thermally shocked and thermally-shocked composites are shown in Fig. 13. In both of the specimens the load increased linearly in the initial stage and after the load had reached its maximum value, the load decreased gradually with increasing displacement. This load–displacement behaviour was completely independent of whether or not the specimen was subjected to thermal shock.

The residual flexure strength and Young's modulus versus thermal shock temperature are shown in Fig. 14. As is clearly shown in this figure, a slight

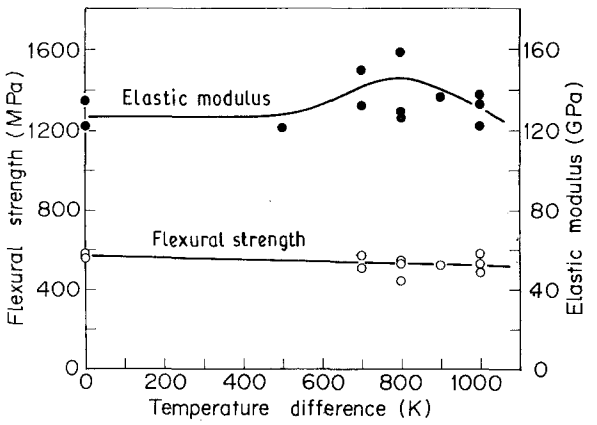

Figure 14 Plots of longitudinal Young's modulus and three-point flexure maximum stress versus thermal shock temperature for SiC fibre-reinforced LAS matrix composite.

decrease of the flexure strength was observed after the thermal shock and the decrease in strength at $\Delta T = 1000$ K from $\Delta T = 0$ (non-thermally shocked composite) was less than 5%. The Young's modulus of the composite increased with increasing thermal shock temperature up to around 800 K and then decreased gradually. The increase of Young's modulus of the composite is well contrasted with the formation of β-spodumen, and therefore the increase is probably due to crystallization of the LAS matrix, i.e. formation of β-spodumen. The decrease in the Young's modulus is due to microcracking of the LAS matrix.

4. Conclusions

The results of thermal shock experiments showed that the damage of the composite differed with the matrix materials used. The results are as follows.

1. For the borosilicate glass matrix, multiple cracking of the matrix perpendicular to the fibre axis occurred only near the surface. Decrease in both flexure strength and Young's modulus occurred at thermal shock temperatures higher than 600 K. This behaviour seems strongly related to the multiple cracking phenomenon of the matrix. The decrease in the strength was due to the change of fracture mode and a higher probability of interlaminar shear fracture reduced flexure strength.

2. For the LAS matrix composite, microcracking of the matrix by thermal shock treatment occurred only at the surface of the composite and this behaviour was independent of thermal shock temperatures higher than 800 K. The microcracks formed parallel to the fibre axis. Although microcracking was formed in the matrix, the flexure strength of the composite was nearly the same as the original strength level. Young's modulus of the composite decreased when the matrix underwent microcracking, and the microcracking behaviour seems to be strongly dependent on the formation of β-spodumen-silica solid solution in the matrix. It is concluded that the SiC fibre-reinforced LAS matrix composite possesses a high resistance to thermal shock at temperatures below 800 K.

3. A clear understanding of the microcracking behaviour seems to be important in understanding degradation of the fibre-reinforced ceramics. It is concluded that the advantage of the composite against thermal shock is considered to be non-catastrophic failure resulting from fibre toughening. Further experiments are required for the quantitative understanding of the thermal shock behaviour in fibre-reinforced ceramics.

Acknowledgements

The authors thank Dr H. Ichikawa and Dr Y. Imai, Nippon Carbon Corporation, for their help with processing of the composite material. The part of a paper presented at the 13th Annual Conference on Composites and Advanced Ceramic Materials, 15-18 January 1989, Cocoa Beach, FL, USA, sponsored by the Engineering Ceramics Division, The American Ceramic Society, Inc.

References

1. K. M. PREWO, *J. Mater. Sci.* **17** (1982) 3549.
2. K. MARSDEN, *J. Metals* July (1987) 30.
3. L. S. MILLBERG, *ibid.* November (1987) 10.
4. A. S. FAREED, M. J. KOCZAK, F.KO, and G. LAYDEN, in "Advances in Ceramics", Vol. 22, "Fractography of Glass and Ceramics" (American Ceramic Society, Westerville, (1988) pp. 261-78.
5. K. S. MAZDIYASNI and R. RUH, *J. Amer. Ceram. Soc.* **64** (1981) 415.
6. J. M. YANG, J. C. CHOU, and C. V. BURKLAND, in Materials Research Society Symposium Proceedings, Vol. 120, "High Temperature/High Performance Composites", edited by F. D. Lemkey, S. G. Fishman, A. G. Evans, and J. R. Strife (MRS, 1988) pp. 163-8.
7. M. C. LONG, R. E. MOORE, D. E. DAY, J. G. WESLING, and R. BURNS, *Ceram Engng Sci. Proc.* **10** (1989) 1231.
8. K. HONDA and Y. KAGAWA, *J. Jpn. Inst. Metals* **54** (1992) 481.
9. G. A. COOPER and J. M. SILLWOOD, *J. Mater. Sci.* **7** (1972) 325.
10. S. R. LEVITT, *ibid.* **8** (1973) 739.
11. K. M. PREWO, in "Tailoring Multiphase and Composite Ceramics", edited by R. E. Tresser, G. L. Messing, C. G. Pantano and R. Newnham (Plenum, New York, 1986) pp. 529-47.

Received 2 September 1991
and accepted 17 June 1992